Journal of Radiation Research and Applied Sciences 15 (2022) 32–43

Contents lists available at ScienceDirect

Journal of Radiation Research and Applied Sciences

journal homepage: www.journals.elsevier.com/journal-of-radiation-research-and-applied-sciences

Development of a computer-aided tool for detection of COVID-19 pneumonia from CXR images using machine learning algorithm

Nurul Absar [a], Baitul Mamur [a], Abir Mahmud [a], Talha Bin Emran [b], Mayeen Uddin Khandaker [c,*], M.R.I. Faruque [d], Hamid Osman [e], Amin Elzaki [e], Bahaaedin A. Elkhader [e]

[a] Department of Computer Science and Engineering, BGC Trust University Bangladesh, Chittagong, 4381, Bangladesh
[b] Department of Pharmacy, BGC Trust University Bangladesh, Chittagong, 4381, Bangladesh
[c] Centre for Applied Physics and Radiation Technologies, School of Engineering and Technology, Sunway University, Bandar Sunway, 47500, Selangor, Malaysia
[d] Space Science Center, Universiti Kebangsaan Malaysia, 43600, Bangi, Selangor, Malaysia
[e] Department of Radiological Sciences, College of Applied Medical Sciences, Taif University, Taif, 21944, Saudi Arabia

A R T I C L E I N F O

Keywords:
COVID-19
X-ray imaging
SVM model
Object detection
CAT platform

A B S T R A C T

The novel coronavirus (SARS-CoV-2) is spreading rapidly worldwide, and it has become a greater risk for human beings. To curb the community transmission of this virus, rapid detection and identification of the affected people via a quick diagnostic process are necessary. Media studies have shown that most COVID-19 victims endure lung disease. For rapid identification of the affected patient, chest CT scans and X-ray images have been reported to be suitable techniques. However, chest X-ray (CXR) shows more convenience than the CT imaging techniques because it has faster imaging times than CT and is also simple and cost-effective. Literature shows that transfer learning is one of the most successful techniques to analyze chest X-ray images and correctly identify various types of pneumonia. Since SVM has a remarkable aspect that tremendously provides good results using a small data set thus in this study we have used SVM machine learning algorithm to diagnose COVID-19 from chest X-ray images. The image processing tool called RGB and SqueezeNet models were used to get more images to diagnose the available data set. Our adopted model shows an accuracy of 98.8% to detect the COVID-19 affected patient from CXR images. It is expected that our proposed computer-aided detection tool (CAT) will play a key role in reducing the spread of infectious diseases in society through a faster patient screening process.

1. Introduction

The continuing coronavirus pandemic has had a feasting dominance on the well-being of the global population and health (Karim et al., 2020). On November 23, 2020, approximately 49,667,976 confirmed cases and 15248,785 deaths cases 35,254,953 recovered cases are reported by Worldometers.info (Worldometers.info, 2020). Within a formation time of 14 days, the syndromes of the disease simulate symbolic toxicity with the respiratory taint (Bell & Murphy, 2022). Current studies state that COVID-19 is often induced by intense keen respiratory ailment SARS-CoV-2 (Li et al., 2020a). It has been reported that the mean incubation period and the mean serial interval are 5.2 days and 7.5 days, respectively, and on average, a SARS-CoV-2 carrier can spread it to ~2.2 persons (Li et al., 2020a). In meeting the rising number of patients, the hospitals must be scaled up their capacities, which poses a big challenge to many governments worldwide (https://covid19.who.int/). Therefore, to reduce the spread of SARS-CoV-2, it is necessary to develop fast screening methods to rapidly identify the COVID-19 cases and then segregate them from other conditions (Wang and Wong, 2020).

In the case of molecular diagnostics, the real-time (quantitative) reverse transcriptase-polymerase chain reaction (RT-PCR) is a widely used diagnostic method. At present, this method shows extensive use in diagnosing COVID-19, which detects amplified SARS-CoV-2 genome in sputum, oropharyngeal swabs or nasopharyngeal, nasal aspirate, bronchoalveolar lavage fluid, and lower respiratory tract aspirates. Although RT-PCR provides sensitive and quantitative detection of the SARS-CoV-2, it is a complex process, requires qualified clinical laboratory personnel, and takes an analysis time of 4–6 h, a sampling-to-result time of around 24 h (Thejeshwar et al., 2020). Moreover, a single RT-PCR test kit may cost more than 50 USD (Ramdas et al., 2020). In addition,

Peer review under responsibility of The Egyptian Society of Radiation Sciences and Applications.
* Corresponding author.
E-mail address: mayeenk@sunway.edu.my (M.U. Khandaker).

https://doi.org/10.1016/j.jrras.2022.02.002
Received 23 August 2021; Received in revised form 4 February 2022; Accepted 6 February 2022
Available online 14 February 2022

sufficient numbers of test kits of RT-PCR are not available in many countries. So, an automatic detection system is needed to be implemented as a quick alternative diagnosis option to prevent the spread of COVID-19 among people (Thejeshwar et al., 2020).

According to the World Health Organization, COVID-19 showed symptoms like SARS. It creates holes in the lungs, generic them a “honeycomb-like appearance” (https://www.nationalgeogr, 2020; Zhang, 2020). Therefore, several studies were performed to detect COVID-19 cases using chest X-ray (CXR) and computed tomography (CT) images as a relatively rapid detection technique. However, based on the X-ray and CT images, the radiologists often find difficulties in accurately identifying COVID resulting from pneumonia from other pulmonary disorders and community-acquired pneumonia (Li et al., 2020b). As a result, artificial intelligence is attractive to both researchers and clinicians for the timely detection of COVID-19 patients (Ozsahin et al., 2020). In this regard, many researchers collected radiographic data from the open-source COVID-19 database and analyses accordingly (Chung, 2020a, 2020b; Cohen et al., 2020). Machine learning and deep learning techniques have been used to identify abnormal patterns of X-ray and CT images (Kumar et al., 2020). Generally, machine or deep learning techniques and several classical image processing tools are used to naturally categorize the diseases with the digitized version of CXR images (Baltruschat et al., 2019; Rahmat et al., 2018). In this connection, many researchers tested the potential of Convolutional Neural Network (CNN) (Apostolopoulos & Mpesiana, 2020; Chowdhury et al., 2020a,; Hemdan et al., 2020; Narin et al., 2020a) by using the existing CNN architectures such as AlexNet, ResNet, Dense Net, Google Net, VGG, Xception, Inception, ResNet, and MobileNet. Note that CNN architecture is produced to develop the discrimination capability of the COVID-19 affected region in the chest x-ray images. The concatenated features raise the diversity in the feature space, which is then assigned to the SVM classifier to effectively segregate the COVID-19 infected and non-infected patients.

COVID-19 positive case was detected from CXR images using a deep convolution network with 91.62% classification accuracy (Das et al., 2021). But the study did not include the accuracy of various models for multiclass classification. To identify and manage COVID-19, an efficient and effective tool has to be developed, including multiclass variety. In this connection, the deep learning approaches with some particular features of COVID-19 patients from CXR images show some attention to the scientific community. This is because a screening method based on a chest X-ray image may have many advantages. It may be fast, simultaneously inspect various instances, more accessibility, and utmost significance in clinics with a restrained selection of test tools and facilities. Moreover, the uses of radiology imaging resources are available in almost all hospitals and clinics, making the radiography-based method more accessible and convenient to use. A search of the literature shows that in dealing with the COVID-19, Wang et al. (Wang and Wong, 2020) proposed 19 layers of deep CNN architecture (multi-class classification) based on the idea of ResNet, and named it as COVID-Netby, COVID- and COVID + affected pneumonia patients. The proposed model demonstrated an accuracy of 92%. Afshar et al. (Afshar et al., 2020) introduced COVID-CAPS based on Capsule Net and achieved 80% sensitivity and 98% accuracy (Afshar et al., 2020). Likewise, a pre-trained ResNet-50 model has been applied on a small CXR dataset which showed a 98% accuracy (Narin et al., 2020a). In another study, transfer learning (TL) from a pre-trained inception network was used for the prediction of COVID-19 with an accuracy of 89.5% (Wang et al., 2020a). Narin et al. (Narin et al., 2020b) proposed a neural network for two classes (normal and COVID-19) via a TL technique. The model (ResNet-50) was trained by using only 100 images where 50 images were assigned to each class, and it provides the maximum recognition rate of 98% accuracy. An accuracy of 97% and 87% were reported by the other two proposed models InceptionV3 and Inception-ResNetV2, respectively. Loey et al. (Loey et al., 2020) introduced the TL technique for the training, testing, and validation phase. Pre-trained models and Googlenet, Alexnet, Resnet18 were used for the TL phase. The Generative Adversarial Network (GAN) was used for image preprocessing (Zhong et al., 2015). They have reported a maximum accuracy of 80.6%, 85.2%, and 99.9% using Googlenet (for four classes), Alexnet (for three classes), and Resnet18 (for two classes, covid-19 and normal), respectively. Asmaa et al. (Abbas et al., 2020) presented a classification model for the diagnosis of the COVID-19 from SARS and normal cases and named them as decompose, transfer (transfer learning), and compose (DeTraC). Maximum accuracy of 95.21% was reported in their study. Chowdhury et al. (Chowdhury et al., 2020b) introduced a system based on parallel-dilated CNN to diagnose COVID-19 patients using CXR images and reported a maximum accuracy of 96.58%. Rahimzadeh and Attar (Rahimzadeh & Attar, 2020) proposed a series of ResNet50V2 (He et al., 2016) and Xception (Chollet, 2017) networks as the deep learning model and reported an overall accuracy of 91.4%.

The above literature shows that many artificial intelligence (AI) systems have been proposed based on machine or deep learning, which displayed auspicious accuracy in detecting COVID-19 infected patients via radiography imaging (Arora et al., 2020; Gozes et al., 2020; LeCun et al., 2015; Li et al., 2020c; Shen et al., 2017; Shi et al., 2020; Xu et al., 2020). Among them, support vector machines and random forests are the most applied machine learning methods. At the same time, convolutional neural networks and Long Short-Term Memory are the most deep learning methods used in this regard (Hanumanthu, 2020; Pathan et al., 2020). To the best of our knowledge, no earlier studies have been done using the Support Vector Machine (SVM) model to detect COVID-19 positive and negative cases using CXR images in Bangladesh during the preparation of this manuscript or during this manuscript the study period. Therefore, we have proposed a simple technique to classify COVID-19 positive and negative cases using CXR images, enhancing representational capacity while significantly decreasing the computational complexity.

In Bangladesh, currently, no patient can enter the doctor’s chamber or visit the doctor without having a Chest X-ray image to show the primary condition (COVID positive or negative) if they are suffering from fever and other similar symptoms. Moreover, people have to take an X-ray image after two weeks of suffering from COVID-19 to ensure that they are COVID-19 negative. This is because, in Bangladesh, a CT image is 20–30 times costly than an X-ray and also time-consuming. The same situation is for rt-PCR. Moreover, CT gives a high radiation exposure to the patients. Therefore, considering the local situation/constraints such as economic condition, number of patients in this densely populated country, the overall situation of the healthcare facility, etc., the doctor does not prefer the CT image for primary screening tool though it is used for serious cases. Therefore, the main objective of this study was to develop a computer-aided tool (CAT), which is programmed by a machine-learning algorithm to quickly identify the COVID-19 symptom by the doctor based on an X-ray image. Since COVID-19 is a highly contagious disease, many doctors in Bangladesh are affected by their routine patient dealing activities. So, the motivation of this work is to provide a CAT that helps the doctor to identify/initial screening of COVID-19 Positive or Negative of the incoming patient in the doctor’s chamber. Using this technique, accurate detection of COVID-19 patients can be done within a few seconds through CXR images. Even without the presence of a radiologist, our proposed machine learning-based tool may be able to provide an opinion without the need of human intervention. In this regard, this work presents an automatic COVID-19 CXR image classification system based on a support vector machine. The presented approach is very useful for the clinical professionals for early detection of COVID-19 affected patients.

The structure of the rest of this paper is as follows. Section 2 presents the mathematical formulation of the used SVM model and a workflow of the whole process. The next section explains the experimental results and comparison with the available literature, followed by a conclusion in Section 4.

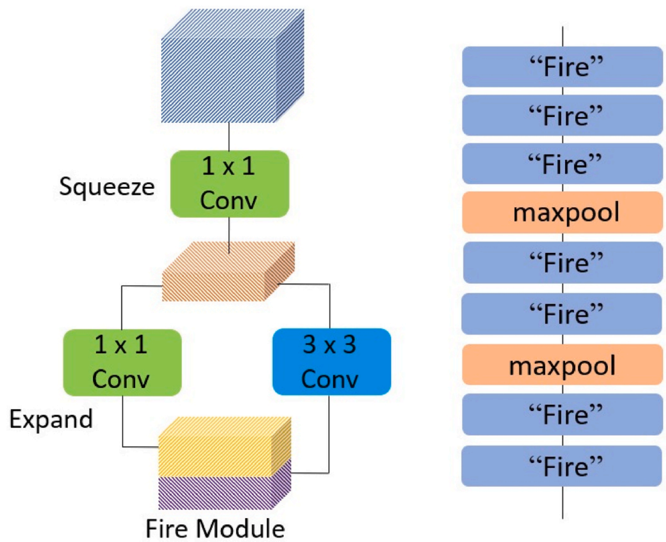

Fig. 1. The architecture of SqueezeNet.

2. Methods

2.1. SqueezeNet

SqueezeNet is a small CNN architecture proposed by (Iandola et al., 2016) whose accuracy is almost AlexNet-level (Krizhevsky et al., 2012). It has 50 times fewer parameters and is 510 times smaller in size than AlexNet, but it has more convolutional layers than the AlexNet. However, it does not mean that the processing time of SqueezeNet would be faster than AlexNet (Bianco et al., 2018). The benefit of SqueezeNet is the use of a small model size which provides less computational complexity. SqueezeNet is an in-depth learning model having an input size of 224 × 224 pixels. It comprises convolutional-, pooling-, ReLU-, and Fire layers. Although it does not have a fully connected layers and dense layers, however, the Fire layers can perform such job. This model uses a 1 × 1 convolutional filter to the input image in the Compression part, and 1 × 1 and 3 × 3 convolutional filters in the Expansion part of the Fire layer. Both the Expansion and Compression parts keep the same feature map size. In the Expansion part the depth of the input image is increased, while in the Compression part, the depth is first reduced and then increased (bottleneck) (Fu et al., 2019; Lee et al., 2019). Down-sample late in the network to facilitate the large activation maps to convolution layers. A simple architecture of the SqueezeNet is given in Fig. 1.

2.2. Data augmentation

When the number of training data set is relatively small which are representative of the test set, then the data augmentation is usually used to increase the data. We applied data augmentation to increase the data including vertical and horizontal reflections, rotation, and shear as per the technique in refs. (Perez & Wang, 2017; Shorten & Khoshgoftaar, 2019). It has been used to improve the generalization of the learning model and to augment the training samples with variations (Shorten & Khoshgoftaar, 2019; Zheng et al., 2020).

2.3. SVM classification

The Support Vector Machines (SVM) is a supervised machine learning algorithm that can be used for both regression challenges and sorting (Cortes & Vapnik, 1995; Theodoridis & Koutroumbas, 2003; Vapnik, 1998). Many studies are available using Machine Learning SVM, primarily, to solve Classification problems. The SVM algorithm aims to make the best line or decision boundary named hyperplane which can set apart n-dimensional space into classes, and then one can easily insert the new data in the correct category in the upcoming work. To create the decision boundary, SVM chooses the extreme points. These ultimate cases are named as support vectors, and hence algorithm is termed as SVM. In this algorithm, considering the value of each property as the value of a particular coordinate, each data item is divided as a point in n-dimensional space. After that, we execute classification by finding the hyperplane that differentiates the two classes very well. SVM is very effective in large dimensional spaces. The SVM is implemented by the use of the scikit-learn package in python. The pre-processed data is divided into 30% test data and 70% training data. A hyperplane or group of hyperplanes in a high- or infinite-dimensional space is constructed by an SVM. A good separation is accomplished by the hyperplane which has the greatest distance to the nearest training data point of any class (Fig. 2). SVM aims to get an optimal hyperplane that divides the data into different classes. Relevant theoretical information or mathematical formulation is given as follows.

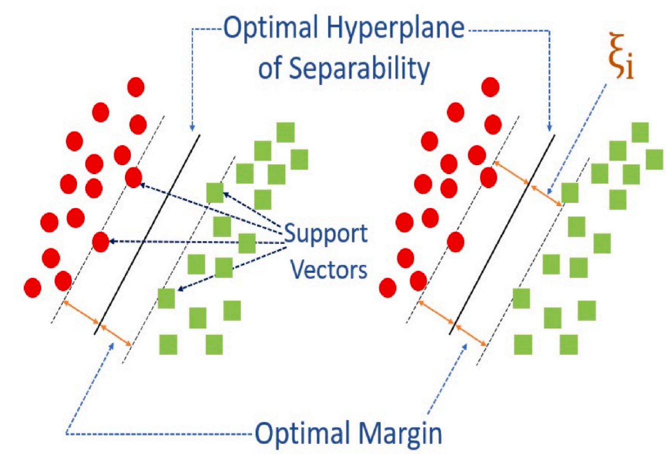

Fig. 2. Linear and nonlinearly separable classes with ξ measure the error of the hyperplane fitting (Vapnik, 1998).

Suppose the training data are represented by $\{x_i, y_i\}$, i = 1, 2, …, N, and y_i ε {-1, +1}, where the number of training samples is denoted by N, $y_i = +1$ for class ω_1 and $y_i = -1$ for class ω_2. Let us consider the two classes are linearly divisible. So, it is possible to get at least one hyperplane defined by a vector *w* with a bias $w_0$which can separate the classes without error:

$$f(x) = w.x + w_0 = 0 \tag{1}$$

To get such a hyperplane, *w* and w_0 should be expected in a way that $y_i\,(w.x_i + w_0) \geq 1$ for $y_i = +1$ (class ω_1) and $y_i\,(w.\,x_i + w_0) \leq -1$ for y_i = -1 (class ω_2). To get equation (2), these two can be added to provide

$$y_i(\,w.x_i + w_0) - 1 \geq\ 0 \tag{2}$$

The support vectors must be identified to find the optimal hyperplane. There are two hyperplanes that are parallel to the optimal are laid on the support vectors which is given below:

$$w.x_i + w_0 = \pm 1 \tag{3}$$

If *w* and w_0 are taken by a simple rescaling of the hyperplane parameters, the margin can be expressed as $\frac{2}{W}$

After solving the following optimization problem, we get the optimal hyperplane

$$Minimize\ \frac{1}{2W^2}$$

Subject to $y_i(\,w.x_i + w_0\,) - 1 \geq 0;\ i\ = 0, 1, 2, 3, \ldots\ldots\ldots..N$

The above problem can be translated to by using a Lagrangian formulation,

$$Maximize \sum_{i=1}^{N}\lambda_i - \frac{1}{2}\sum_{i,j=1}^{N}\lambda_i\lambda_j y_i y_j (x_i x_j) \tag{4}$$

Subject to. $\sum_{i=1}^{N}\lambda_i y_i = 0 \; and \; \lambda_i \geq 0; \; I = 0,1,2,3,\ldots\ldots\ldots\ldots\ldots N$

Where the Lagrange multipliers are denoted by λ_i. We got the optimal hyperplane discriminant function under this formulation which is:

$$f(x) = \sum_{i\epsilon S}^{N}\lambda_i y_i (x_i x) + w_0 \tag{5}$$

Here, a subset of training samples is denoted by S that corresponds to non-zero Lagrange multipliers.

In most of the terms, classes are not linearly separable, and the constraints of equation (2) cannot be satisfied. So in those terms, a cost function can be defined to combine minimization of error criteria and maximization of margin by using several variables called slack variables ξ (Fig. 1). This cost function is defined as:

$$Minimize \; J(w, w_0, \xi) = \frac{1}{2W^2} + C\sum_{n=1}^{\infty}\xi_i \tag{6}$$

Subject to $y_i(\, w.x_i + w_0) \geq 1 - \xi_i; \; i = 0,1,2,3,\ldots\ldots\ldots\ldots\ldots N$

According to Mercer's theorem (Chandrakala & Sumathi, 2014; Hsu & Lin, 2002; Mercier & Lennon, 2003), the inner product of the vectors in the mapping space can be expressed as a function of the inner products of the corresponding vectors in the model space. The following equivalent representation has been used for inner product operation:

$$\phi(x)\phi(z) = K(x, z) \tag{7}$$

Where, a kernel function is denoted by K (x,z) which is used for training without knowing the ϕ as explicit form. The dual optimization problem is now stated as:

$$Maximize \sum_{i=1}^{N}\lambda_i - \frac{1}{2}\sum_{i,j=1}^{N}\lambda_i\lambda_j y_i y_j K\,(x_i x_j) \tag{8}$$

Subject to $\sum_{i=1}^{N}\lambda_i y_i = 0 \; and \; \lambda_i \geq \; 0 \; ; \; i = 0,1,2,3,\ldots\ldots\ldots\ldots N$

Therefore, the output classifier becomes:

$$f(x) = \sum_{i\in S}\lambda_i y_i K(x_i x) + \; w_0 \tag{9}$$

2.4. SVM multi-class classification

Two main approaches have been suggested for implementing SVM into multi-class classifications. The first approach is named "one against all". Though it is a quick method, by marginally imbalanced training sets errors are occurred. The N decision functions using equation (9) is not possible to find that the problem of optimization was currently introduced (Donahue et al., 2014), which is much related to the "one against all" method. The second approach is known as "one against one". It is very much used to solve multi-class classification problems due to the demanding computation than the "one against all" method (Donahue et al., 2014).

2.5. Concept diagram

The workflow of the proposed method is given as follows. Firstly, the CXR images are extracted from open-source databases and used as training samples. The images were then augmented to enhance the classification performance and resized to a similar size. To extract features and perform the classification, the transfer learning technique is employed in the images. Lastly, unknown test images are supplied to the

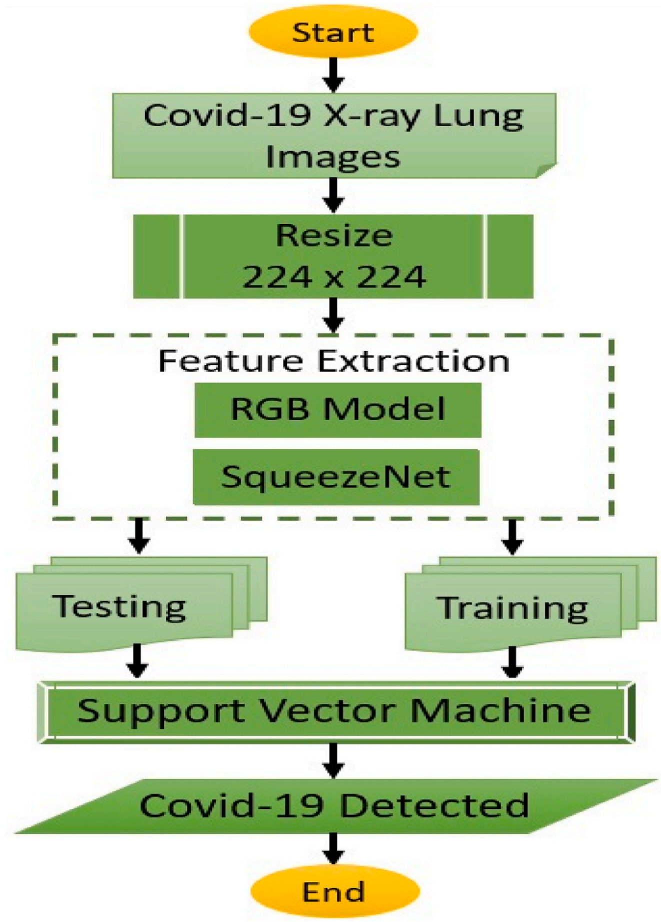

Fig. 3. Workflow of the system for the identification of COVID-19 patients.

network to evaluate the performance by calculating the proposed method's accuracy, precision, recall, and F1-score. Our proposed system is shown in Fig. 3. In this analysis, we collected patient X-ray data, then added the data to the system. Admin shows the details of the patients. The system classifies the patient images. Then the result shows the X-ray is COVID-19 positive or negative.

2.6. Texture-feature extraction

The co-occurrence matrix is used to extract texture features. By using equation (10) the input sample is converted into a greyscale image (Chandrakala & Sumathi, 2014).

$$Y_c = \; 0.29 * R_c + 0.589 * G_c + 0.114 * B_c \tag{10}$$

The grayscale value is denoted by Yc, Red component is denoted by Rc, the Green component is denoted by Gc, Blue component is denoted by Bc. The statistical measure of the Contrast, Energy, Homogeneity, Correlation used for texture features are as follows:

$$Contrast = \sum_{i,j}(i-j)^2 p(i,j) \tag{11}$$

$$Energy = \sum_{i,j}P(i-j)^2 \tag{12}$$

$$Homogenety = \sum_{i,j}\frac{p(i-j)}{1+(i-j)} \tag{13}$$

$$Correlation = \sum_{i,j}\frac{(i-\mu i)(j-\mu j)p(i,j)}{\sigma_{i\sigma_j}} \tag{14}$$

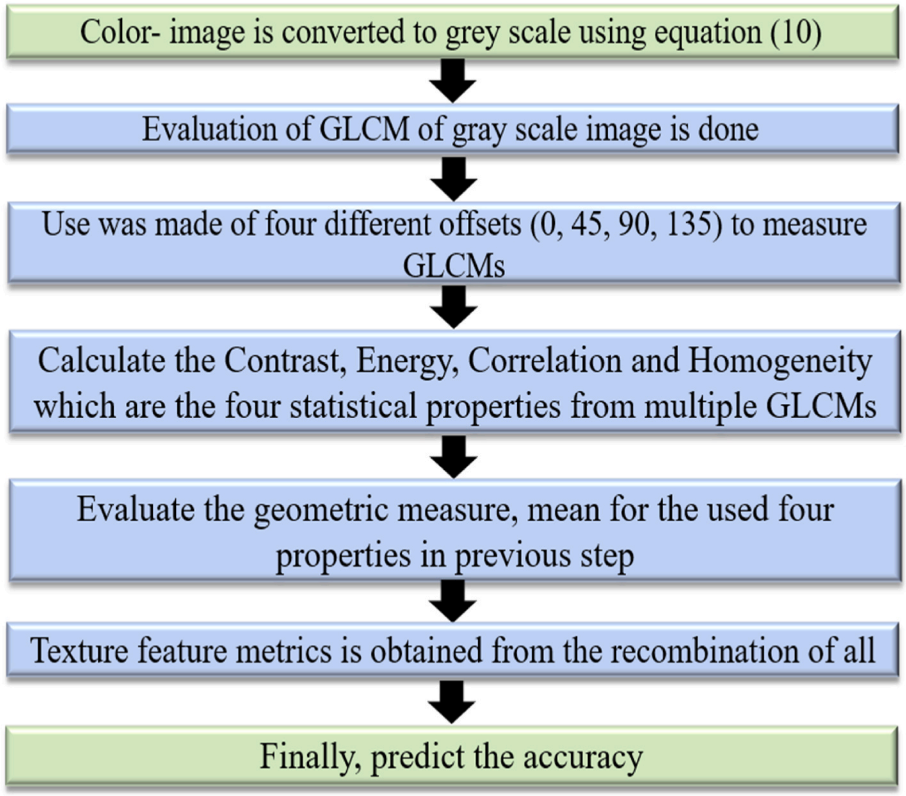

Fig. 4. Step-by-step processes for the extraction of texture-feature.

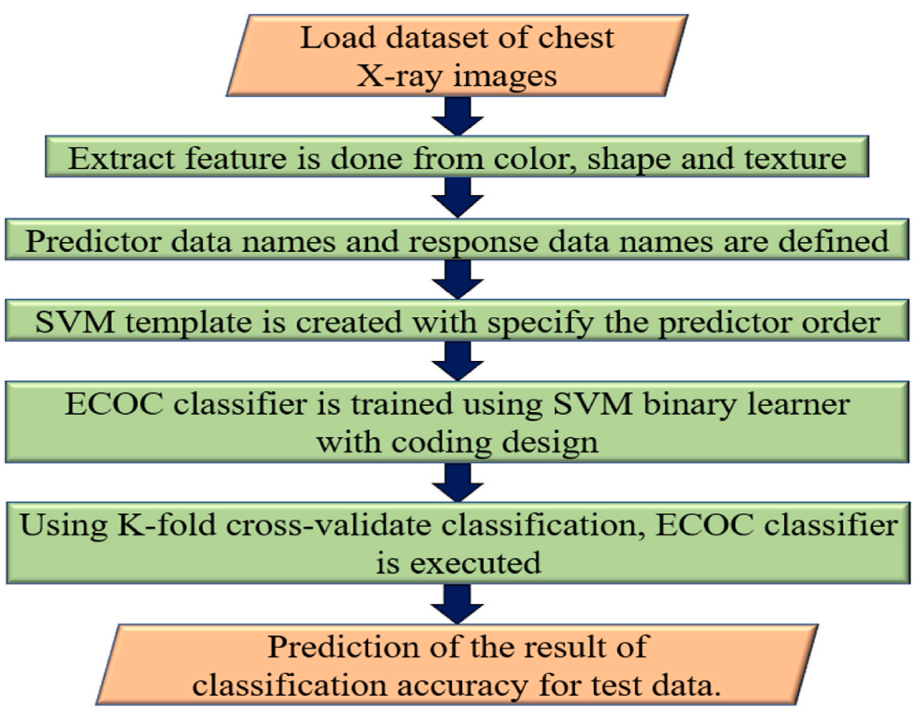

Fig. 5. Step-by-step processes for the execution of ECOC classifier.

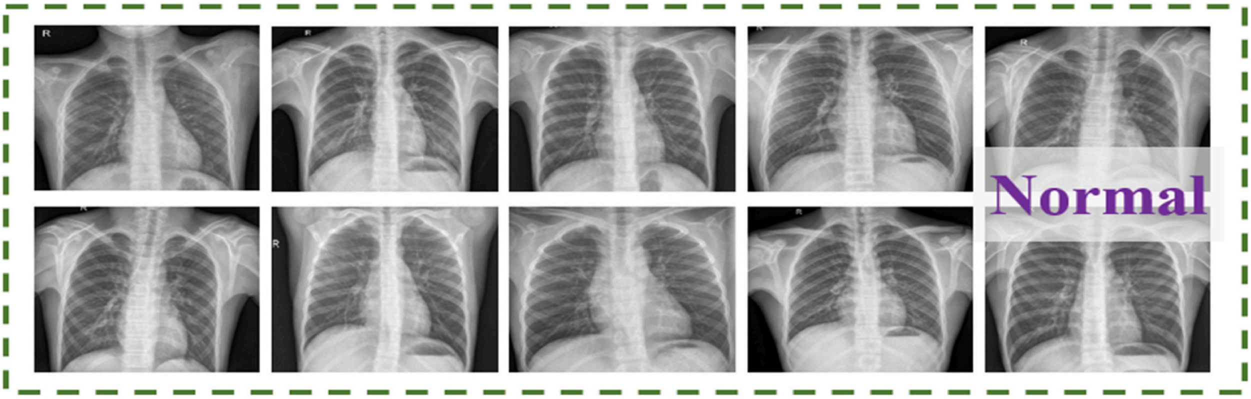

Fig. 6. Sample of the collected dataset: normal Images.

The statistical properties are calculated using equations 11–14. The extraction of texture-feature was considered as follows, as presented in Fig. 4.

2.7. SVM and category sorting using color, shape, texture of training image

We used 7180 chest X-ray images dataset as an input where 619 sample images of COVID-19, 1341 samples of the normal chest X-ray image, and 5220 sample images of viral pneumonia, consisting image size 224 × 224. Then the color, shape, and texture features of the three images were extracted. After that, the image divides into 80% training data and 20% test data, 5 fold cross-validation was performed with the training data here.

2.8. SVM-Eco classification

SVM has been used for classifying points into disjoined planes (Donahue et al., 2014), pattern recognition, and text categorization (Demirkesen & Cherifi, 2008). Nowadays, there is a need for multiclass classification with a big set of data (Dietterich & Bakiri, 1995). In 1995, the Error-correcting output coding (ECOC) framework was proposed by (Yan & Yang, 2014) for converting multiclass into some binary problems. The SVM, when combined with ECOC, enriches the system failure when solving multiclass classification (Fatima & Seshashayee, 2019).

ECOC was used to decrease multiclass problems to a set of binary classifiers which includes two schemes. The first one is the Coding Scheme, where the coding design presents the ways through a multiclass problem which is reduced to a group of binary class problems. The second one is the Decoding Scheme, which shows the ways to merge result that was obtained from binary learners (Error correcting output c, 2019; https://in.mathworks.com/, 2019). The Block diagram of SVM-ECOC is presented in Fig. 5.

2.9. Train and predict function

By using the template SVM (Nixon & Aguado, 2013) function, we created a model that returns a support vector machine template that is applicable to train ECOC multiclass. The entity of this SVM template consists of some options for the classification of SVM. Then, it needs to train the ECOC classifier. So, by using SVM binary learners with a one-vs-one coding design, the ECOC classifier gets trained. ECOC multiclass learning is done by using 'fitcecoc' function (https://in.mathworks.com/, 2019).

2.10. Accuracy measurements

Accuracy is commonly used as a classification metric (Dietterich & Bakiri, 1995). The classification metrics depend on the domain area and technique used. The prediction accuracy was measured by using the following equation (Chowdhury et al., 2020a).

$$\text{Accuracy} = \frac{\text{TP} + \text{TN}}{(\text{TP} + \text{FP} + \text{FN} + \text{TN})} \tag{15}$$

Where TP, FP, TN, and FN represent the true positive, false positive, true negative, false negative, respectively.

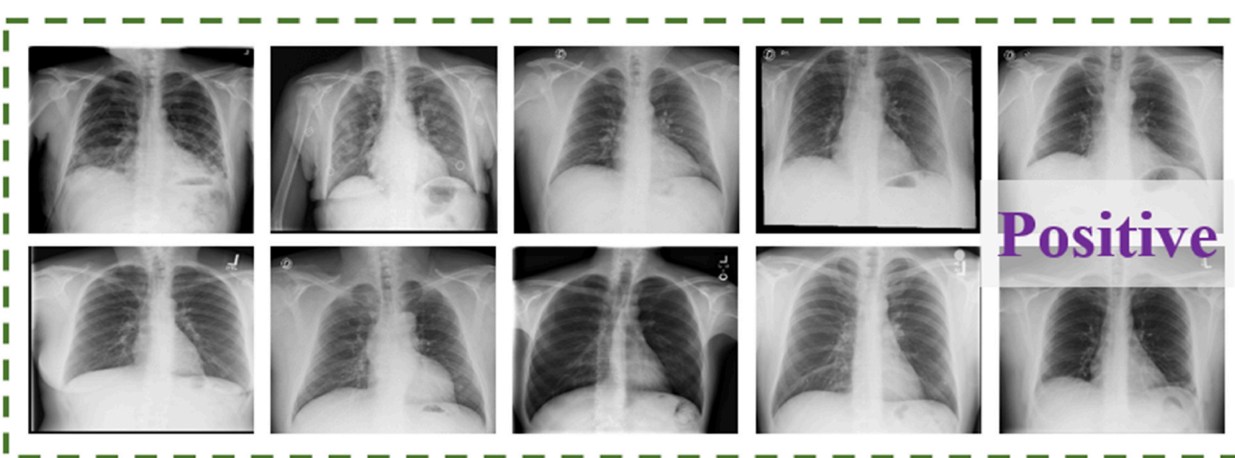

Fig. 7. Sample of the collected dataset: COVID Positive Images.

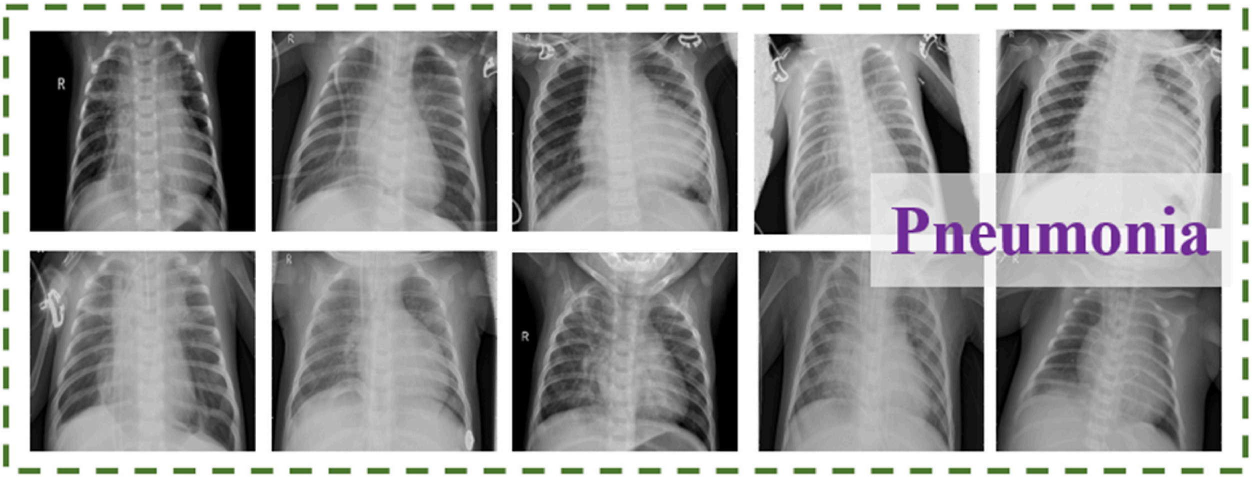

Fig. 8. Sample of the collected dataset: Pneumonia Images.

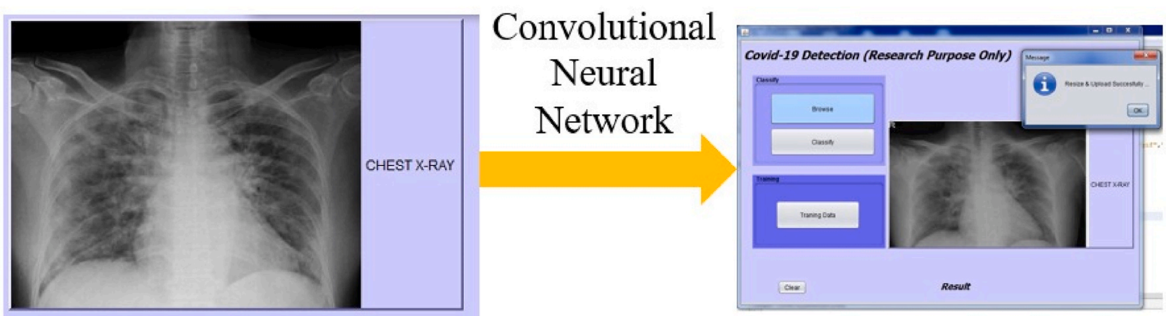

Fig. 9. X-Ray image before and after resizing.

3. Experimental results and discussion

3.1. Model RGB and resizing

In this study, we have extracted the images from various open-source databases. They contain X-Ray images of COVID-19 patients, normal and viral pneumonia where 619 sample images of COVID-19, 1341 normal chest X-ray images, and 5220 sample images of viral pneumonia (Chowdhury et al., 2020a; https://www.kaggle.com/pa, 2021; https://www.kaggle.com/an, 2021). The samples are given in Figs. 6–8

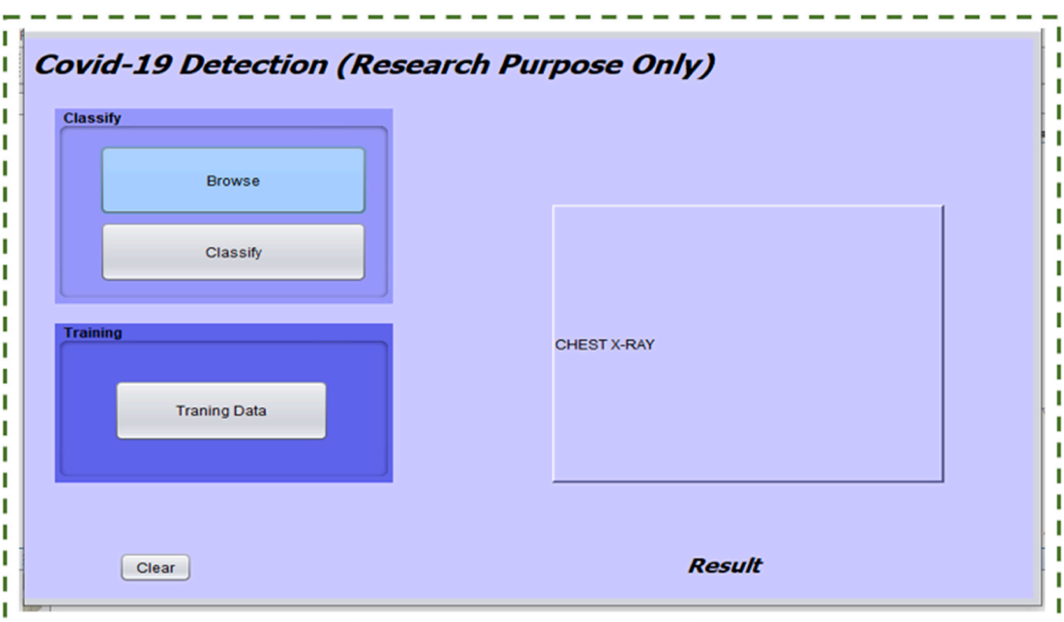

Fig. 10. Home page of the CAT platform.

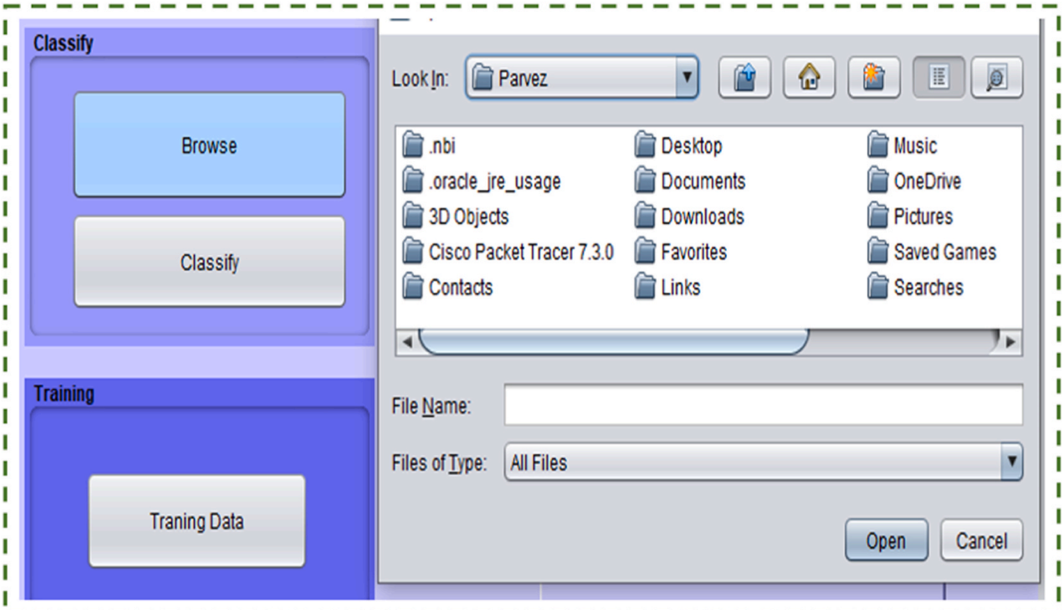

Fig. 11. Dataset folder.

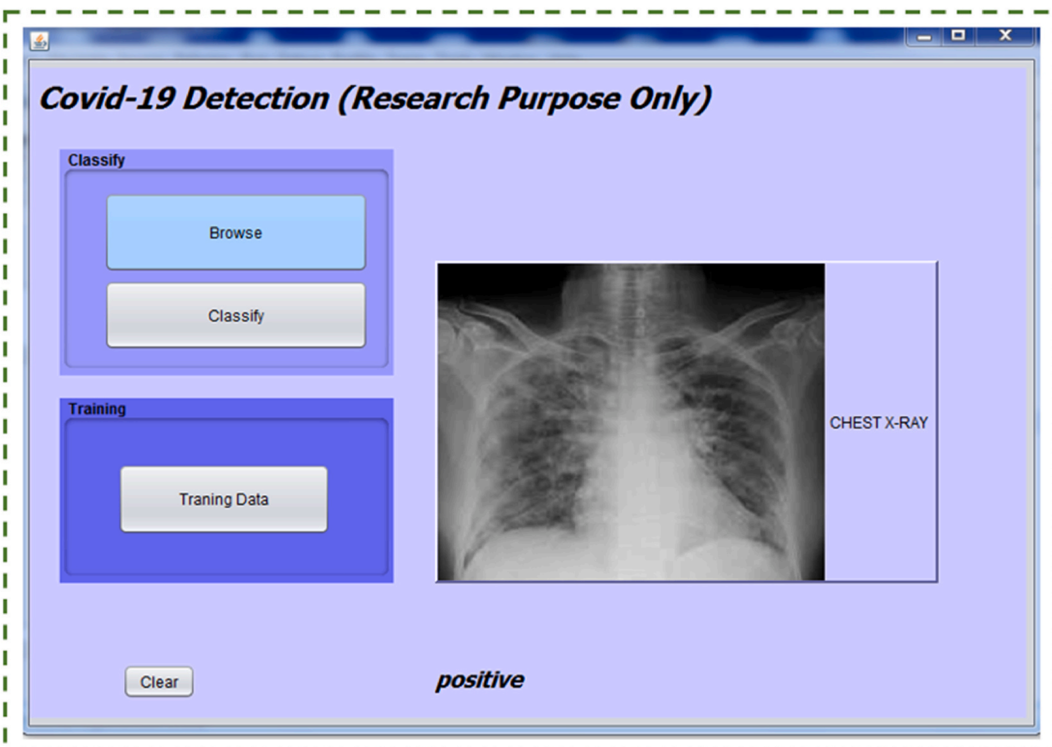

Fig. 12. Positive image classification.

for normal CXR images, COVID-19, and images of viral pneumonia respectively.

However, in this work, the images were segregated into two categories - COVID-19 positive and COVID-19 negative. First, the consolidated images were normalized and resized into 224 × 224 shaped images. Then the images are shuffled and split into training and testing data. A sample of x-ray images before and after resizing is shown in Fig. 9. Where COVID-19 was positive and COVID-19 negative both the test size is 20%, and 80% was for training purposes. However, if there are 2 or more images from the same patient, it is ensured that those images are either marked as training or test data - but not in both. The same patient's image is kept in both the training and test data, however, there is a possibility that the results are overly promising because of patients' overlap. In this way, the images are made available for training the model followed by testing the efficacy of the trained model.

The input file can be classified as the SVM and CSV files. Although the images are conceptualized as rectangular arrays of RGB triplets manipulate in our programs, they are not generally created, stored, or transmitted in that format. The CSV file is the most important for the dataset which can be expressed the position of the patient.

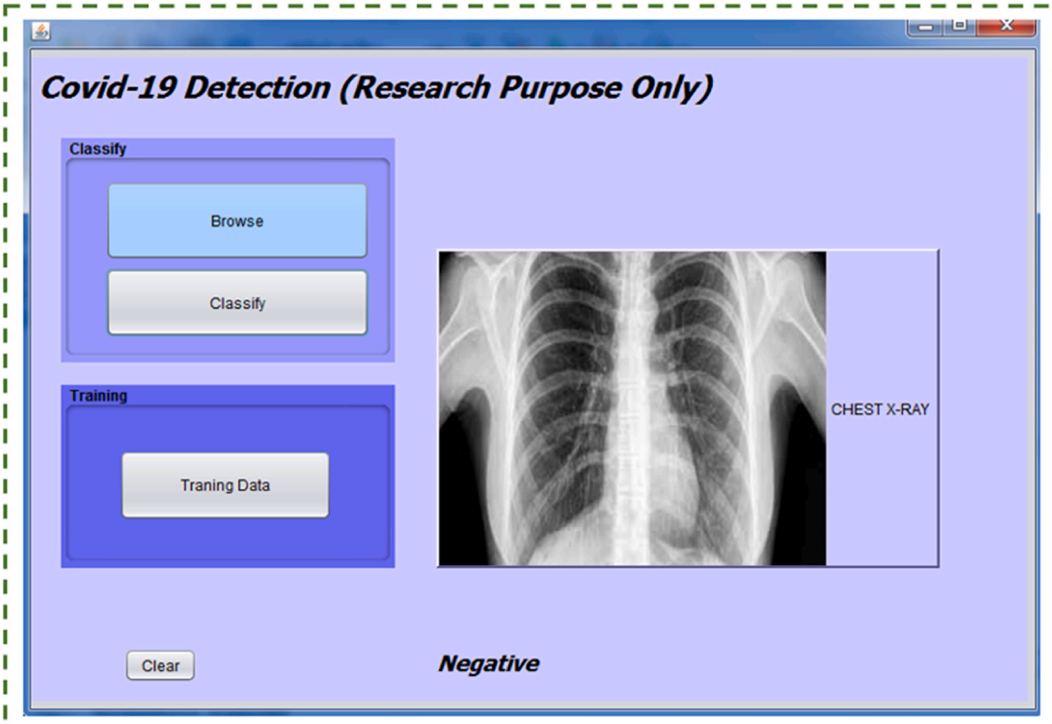

Fig. 13. Negative image classification.

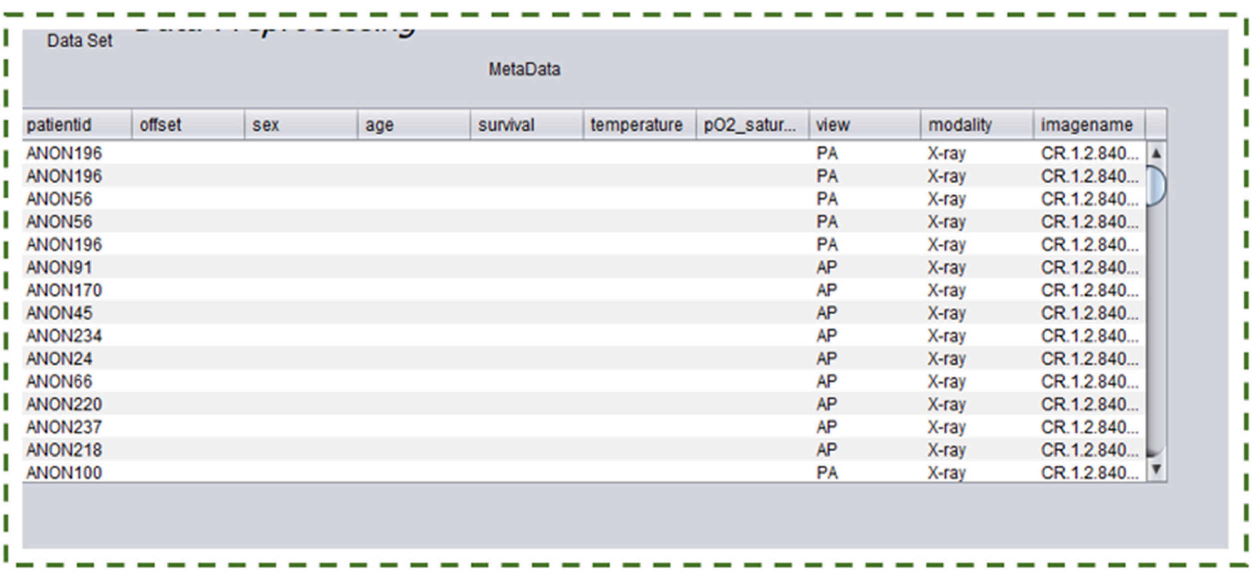

patientid	offset	sex	age	survival	temperature	pO2_satur...	view	modality	imagename
ANON196							PA	X-ray	CR.1.2.840...
ANON196							PA	X-ray	CR.1.2.840...
ANON56							PA	X-ray	CR.1.2.840...
ANON56							PA	X-ray	CR.1.2.840...
ANON196							PA	X-ray	CR.1.2.840...
ANON91							AP	X-ray	CR.1.2.840...
ANON170							AP	X-ray	CR.1.2.840...
ANON45							AP	X-ray	CR.1.2.840...
ANON234							AP	X-ray	CR.1.2.840...
ANON24							AP	X-ray	CR.1.2.840...
ANON66							AP	X-ray	CR.1.2.840...
ANON220							AP	X-ray	CR.1.2.840...
ANON237							AP	X-ray	CR.1.2.840...
ANON218							AP	X-ray	CR.1.2.840...
ANON100							PA	X-ray	CR.1.2.840...

Fig. 14. Datasets.

3.2. Model SVM and detection

Based on this study, a simple desktop tool has been developed for finding COVID-19 positive and COVID-19 negative cases. This allows any medical personnel to browse a CXR image and feed it to the application. The application will then execute the proposed model, and provide the label for the given CXR image. As a result, this will detect the COVID-19 positive and COVID-19 negative cases, as shown in Figs. 8 and 9, respectively. The developed tool can be executed on Windows. This interface can be used in any healthcare facility for fast detection of the COVID-19 patient. The successful implementations have been made as per the following Figs. 10–15.

Table 1 shows that previous studies (Wang et al., 2020b; Minaee et al., 2020, p. P1; Karim et al., 2021; Saiz, 2020 ; Khan et al., 2020; Mohammed et al., 2021) have achieved the minimum accuracy of 91% for multicenter osteoarthritis studies using chest x-ray images, and the maximum accuracy of 98.3% for COVID-RENet and COV-VGGNet models. Some other authors (Ying et al., 2020; Farid et al., 2020) reported a maximum accuracy of 94% for CT images using the DRENet model and lower accuracy of 76.47% for the JRIP model. According to Table 1, Minaee et al. (Minaee et al., 2020, p. P1) and Khan et al. (Khan et al., 2020) used deep learning techniques and found a maximum accuracy of 98% and 98.3%, respectively. On the other hand, the authors (Rini and Rimuljo et al., 2020; Kumar Sethy et al., 2020; Mahdy et al., 2020; Ismael & Şengür, 2021) used SVM with different CNN models to predict the COVID19 from the chest x-ray images and reported a

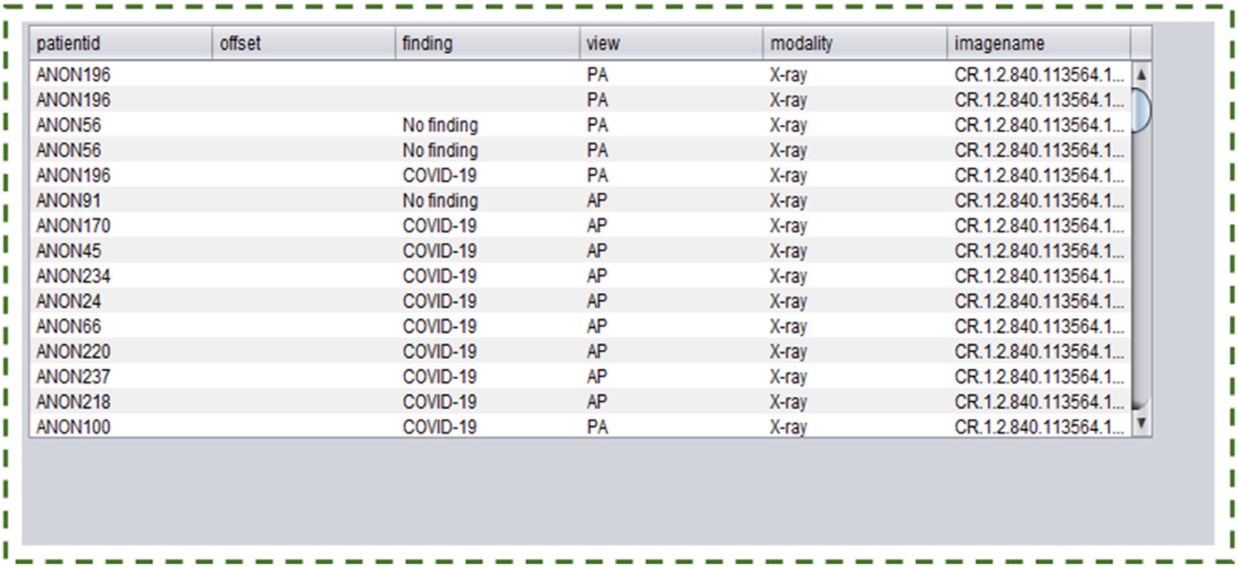

patientid	offset	finding	view	modality	imagename
ANON196			PA	X-ray	CR.1.2.840.113564.1...
ANON196			PA	X-ray	CR.1.2.840.113564.1...
ANON56		No finding	PA	X-ray	CR.1.2.840.113564.1...
ANON56		No finding	PA	X-ray	CR.1.2.840.113564.1...
ANON196		COVID-19	PA	X-ray	CR.1.2.840.113564.1...
ANON91		No finding	AP	X-ray	CR.1.2.840.113564.1...
ANON170		COVID-19	AP	X-ray	CR.1.2.840.113564.1...
ANON45		COVID-19	AP	X-ray	CR.1.2.840.113564.1...
ANON234		COVID-19	AP	X-ray	CR.1.2.840.113564.1...
ANON24		COVID-19	AP	X-ray	CR.1.2.840.113564.1...
ANON66		COVID-19	AP	X-ray	CR.1.2.840.113564.1...
ANON220		COVID-19	AP	X-ray	CR.1.2.840.113564.1...
ANON237		COVID-19	AP	X-ray	CR.1.2.840.113564.1...
ANON218		COVID-19	AP	X-ray	CR.1.2.840.113564.1...
ANON100		COVID-19	PA	X-ray	CR.1.2.840.113564.1...

Fig. 15. Training dataset.

Table 1
Comparison of accuracy for different models for x-ray and CT images.

SL No.	Used Model	Image Type	Accuracy (%)	References
1.	COVID-Net	Chest X-ray Image	93.3	Wang et al. (2020b)
2.	SqueezeNet	Chest X ray Image	98	Minaee et al. (2020)
	ResNet18		98	Minaee et al. (2020)
	ResNet50		98	Minaee et al. (2020)
	DenseNet-121		98	Minaee et al. (2020)
3.	Multicenter Osteoarthritis Study	Chest X-ray Image	91	Karim et al. (2021)
4.	SDD300 model	Chest X-ray Image	94.92	Saiz (2020)
5.	COVID-RENet model	Chest X-ray images	98.3	Khan et al. (2020)
	COV-VGGNet model		98.3	Khan et al. (2020)
6.	VGG16	CT Image	90	Ying et al. (2020)
	DenseNet		92	Ying et al. (2020)
	ResNet		92	Ying et al. (2020)
	DRENet		94	Ying et al. (2020)
7.	SVM	CT image	84.31	Ying et al. (2020)
	Naïve Bayes		92.15	Farid et al. (2020)
	JRIP		76.47	Farid et al. (2020)
	Random Forest		92.95	Farid et al. (2020)
8.	SVM(Resnet50)	Chest X-ray Image	95.38 to classify 2 classes 97.33 for 3 classes	Rini and Rimuljo et al. (2020)
9	SVM(Resnet50)	Chest X ray Image	95.33	Kumar Sethy et al. (2020)
	SVM(LBP)		93.4	
10	SVM(multi-level thresholding)	Chest X-ray Image	97.48	Mahdy et al. (2020)
11	SVM(Resnet50)	Chest X ray Image	94.7	Ismael & Şengür (2021)
12	SVM(GLSZM)	CT image	99.68	Waleed Salehi et al. (2020)
13	SVM	Chest X ray Image	95	Mohammed et al. (2021)
14	SVM(Proposed)	Chest X-ray images	98.8	This work

maximum accuracy of 97.48% (Mahdy et al., 2020). Furthermore, a study entitled 'COVID-DeepNet: Hybrid Multimodal Deep Learning System for Improving COVID-19 Pneumonia Detection in Chest X-ray Images' was carried out in (Al-Waisy et al., 2021), and reported a detection accuracy of 99.93 percent. Mohammed et al. (Mohammed et al., 2020) performed a benchmarking study on the selection of methodology for optimal COVID-19 diagnostic model based on machine learning technique. In that study, they employed the SVM (linear) classifier, which yielded a closeness coefficient of 98.99%. Beside this, in a further study, Al-Waisy et al. (Al-Waisy et al., 2020) reported a detection accuracy of 99.99% for the chest X-ray images using COVID-CheXNet system with hybrid learning model.

Note that, deep learning is a sophisticated and mathematically complex part of machine learning. Applications of deep learning use a layered structure of algorithms that analyze data with a logic structure similar to how a human would conclude. In the present study, we used a simple SVM machine learning algorithm to analyze and interpret data, then learn from it. In fact, in the machine learning technique, the learning process follows a simple linear least squares regression process. Finally, based on the obtained training/learning, our adopted SVM provides the decision for the given problem. Overall, the present study with a simple SVM machine learning technique shows a better accuracy of 98.83% than the available literature study.

4. Conclusions

This work has been done to inexpensively detect the COVID-19 positive/negative patients from chest X-ray images. A very useful tool has been developed that uses machine learning classifiers for the effective classification of COVID-19. By uploading the chest X-ray image in our proposed system, any person can check the COVID-19 status. It will help the doctors to detect the affected patients with the help of computer-aided analysis within a few seconds. We do believe that this will significantly add value to the medical field. SVM has a remarkable aspect that tremendously provides good results using a small training set because the support vector is essential only during data training. Using SVM, the study shows the highest accuracy of 98.83% compared to the available literature data that uses both machine and deep learning algorithms. In the future, we will look for better feature extraction and also try for a balanced dataset.

References

Abbas, A., Abdelsamea, M. M., & Gaber, M. M. (2020). *Classification of covid-19 in chest x-ray images using detrac deep convolutional neural network*. arXiv preprint arXiv: 2003.13815.

Afshar, P., et al. (2020). *Covid-caps: A capsule network-based framework for identification of covid-19 cases from x-ray images*. arXiv preprint arXiv:2004.02696.

Al-Waisy, A. S., Al-Fahdawi, S., Mohammed, M. A., Abdulkareem, K. H., Mostafa, S. A., Maashi, M. S., Arif, M., & Garcia-Zapirain, B. (2020 Nov 21). COVID-CheXNet: Hybrid deep learning framework for identifying COVID-19 virus in chest X-rays images. *Soft Comput*, 1–16. https://doi.org/10.1007/s00500-020-05424-3

Al-Waisy, A. S., Mohammed, M. A., Al-Fahdawi, S., Maashi, M. S., Garcia-Zapirain, B., Abdulkareem, K. H., Mostafa, S. A., Kumar, N. M., & Dac-Nhuong, Le (2021). COVID-DeepNet: Hybrid multimodal deep learning system for improving COVID-19 pneumonia detection in chest X-ray images. *Computers, Materials & Continua, 67* (No.2), 2409–2429. https://doi.org/10.32604/cmc.2021.012955

Apostolopoulos, I. D., & Mpesiana, T. A. (2020). Covid-19: automatic detection from X-ray images utilizing transfer learning with convolutional neural networks. *Phys Eng Sci Med, 43*, 635–640. https://doi.org/10.1007/s13246-020-00865-4

Arora, N., Banerjee, A. K., & Narasu, M. L. (2020). The role of artificial intelligence in tackling COVID-19. *Future Virology, 15*(11), 717–724. https://doi.org/10.2217/fvl-2020-0130

Baltruschat, I. M., Nickisch, H., Grass, M., Knopp, T., & Saalbach, A. (2019). Comparison of deeplearning approaches for multi-label chest x-ray classification. *Scientific Reports, 9*, 1–10.

Bianco, S., Cadene, R., Celona, L., & Napoletano, P. (2018). Benchmark analysis of representative deep neural network architectures. *IEEE Access, 6*, 64270–64277.

Chandrakala, D., & Sumathi, S. (2014). Image classification based on color and texture features using frbfn network with artificial bee colony optimization algorithm. *International Journal of Computers and Applications, 98*(14), 19–29. https://doi.org/10.5120/17252-7592

Chollet, F. (2017). Xception: Deep learning with depthwise separable convolutions. In *Proceedings of the IEEE conference on computer vision and pattern recognition* (pp. 1251–1258).

Chowdhury, M. E. H., et al. (2020a). Can AI Help in Screening Viral and COVID-19 Pneumonia?. In *IEEE Access* (vol. 8, pp. 132665–132676). https://doi.org/10.1109/ACCESS.2020.3010287

Chowdhury, N. K., Rahman, M. M., & Kabir, M. A. (2020b). Pdcovidnet: A parallel-dilated convolutional neural network architecture for detecting covid-19 from chest x-ray images. *Health Information Science and Systems, 8*(1), 1–14.

Chung, A. (2020a). Figure 1 COVID-19 chest x-ray data initiative. https://github.com/agchung/Figure1-COVID-chestxray-dataset.

Chung, A. (2020b). Actualmed COVID-19 chest x-ray data initiative. https://github.com/agchung/Actualmed-COVID-chestxray-dataset.

Cohen, J. P., Morrison, P., & Dao, L. (2020). *COVID-19 image data collection*. arXiv :2003.

Cortes, C., & Vapnik, V. (1995). Support-vector network. *Machine Learning, 20*, 273–297.

Das, A. K., Ghosh, S., Thunder, S., Dutta, R., Agarwal, S., & Chakrabarti, A. (2021). Automatic COVID-19 detection from X-ray images using ensemble learning with convolutional neural network. *Pattern Analysis & Applications, 24*, 1111–1124.

Demirkesen, C., & Cherifi, H. (2008). A comparison of multiclass SVM methods for real worldnatural scenes. In *International conference on advanced concepts for intelligent VisionSystems* (pp. 752–763). October.

Dietterich, T. G., & Bakiri, G. (1995). Solving multiclass learning problems via error-correcting output codes. *Journal of Artificial Intelligence Research, 2*, 263–286.

Donahue, J., Jia, Y., Vinyals, O., Hoffman, J., et al. (2014). A deep convolutional activation feature for generic visual recognition. In *, Vol. 32. Proceedings of the 31st international conference on machine learning, in PMLR* (pp. 647–655), 1.

Error correcting output codes. https://in.mathworks.com/help/stats/fitcecoc.html. (Accessed 28 November 2019).

Farid, A. A., Selim, G. I., Awad, A. H., & Khater, A. (2020). Novel approach of CT images feature analysis and prediction to screen for orona virus disease (COVID-19). *International Journal of Scientific Engineering and Research, 11*, 82. https://doi.org/10.14299/ijser.2020.03.02

Fatima, S., & Seshashayee, M. (2019). Categorized image classification using CNN features with ECOC framework. *International Journal of Recent Technology and Engineering, 8*(2), 145–150. https://doi.org/10.35940/ijrte.A1937.078219

Fu, G., Sun, P., Zhu, W., Yang, J., Cao, Y., Yang, M. Y., & Cao, Y. (2019). A deep-learning-based approach for fast and robust steel surface defects classification. *Optics and Lasers in Engineering, 121*, 397–405. https://doi.org/10.1016/j.optlaseng.2019.05.005

Gozes, O., et al. (2020). *Rapid AI development cycle for the coronavirus (COVID-19) pandemic: Initial results for automated detection and patient monitoring using deep learning ct image analysis*, Article 05037. arXiv :2003.

Hanumanthu, S. R. (2020). Role of intelligent computing in COVID-19 prognosis: A state-of-the-art review. *Chaos, Solitons & Fractals, 138*, 109947. https://doi.org/10.1016/j.chaos.2020.109947

Hemdan, E. E.-D., Shouman, M. A., & Karar, M. E. (2020). *Covidx-net: A framework of deep learning classifiers to diagnose covid-19 in x-ray images*. arXiv preprint arXiv: 2003.11055.

He, K., Zhang, X., Ren, S., & Sun, J. (2016). Identity mappings in deep residual networks. In *European conference on computer vision* (pp. 630–645). Springer.

Hsu, C.-W., & Lin, C.-J. (2002). A comparison of methods for multiclass support vector machines, 2. In *, Vol. 13. IEEE transactions on neural networks* (pp. 415–425). March.

Iandola, F. N., Song, H., Moskewicz, M. W., Khalid, A., Dally, W. J., & Keutzer, K. (2016). *SqueezeNet: AlexNet-level accuracy with 50x fewer parameters and¡ 0.5 MBmodel size*. arXiv preprint arXiv:1602.07360.

Ismael, A. M., & Şengür, A. (2021). Deep learning approaches for COVID-19 detection based on chest X-ray images. *Expert Systems with Applications, 164*(114054). https://doi.org/10.1016/j.eswa.2020.114054

Karim, M. R., et al. (2021). Deep knee explainer: Explainable knee OA diagnosis from radiographs and magnetic resonance imaging. *Digital Object Identifier, 9*. https://doi.org/10.1109/ACCESS, 39757-3062493, 39780.

Karim, M. R., Döhmen, T., et al. (2020). *Deep COVID explainer: Explainable COVID-19 DiagnosisBased on chest X-ray images*, Article 04582v3. arXiv:2004.

Khan, S., et al. (2020). *Coronavirus disease analysis using chest X-ray images and a novel deep convolutional neural network, preprint*. https://doi.org/10.13140/RG.2.2.35868.64646

Krizhevsky, A., Sutskever, I., & Hinton, G. E. (2012). Imagenet classification with deep convolutional neural networks. *Advances in Neural Information Processing Systems, 1*, 1097–1105. https://doi.org/10.5555/2999134.2999257

Kuamr, R., Arora, et al. (2020). *Accurate prediction of COVID-19 using chest X-ray imagesthrough deep feature learning model with SMOTE and machine learning Classifiers. medRxiv*. https://doi.org/10.1101/2020.04.13.20063461.

Kumar Sethy, P., et al. (2020). Detection of coronavirus disease (COVID-19) based on deep features and support vector machine. *International Journal of Mathematical, Engineering and Management Sciences, 5*(4), 643–651. https://doi.org/10.33889/IJMEMS.2020.5.4.052

LeCun, Y., Bengio, Y., & Hinton, G. (2015). Deep learning. *Nature, 521*, 436–444.

Lee, H. J., Ullah, I., Wan, W., Gao, Y., & Fang, Z. (2019). Real-time vehicle make and model recognition with the residual SqueezeNet architecture. *Sensors, 19*. https://doi.org/10.3390/s19050982

Li, L., et al. (2020c). Artificial intelligence distinguishes COVID-19 from community acquired pneumonia on chest CT. *Radiology*. https://doi.org/10.1148/radiol.2020200905

Li, Q., Guan, X., Wu, P., Wang, X., Zhou, L., & Tong, Y. (2020a). Early transmission dynamics in Wuhan, China, of novel coronavirus-infected pneumonia. *New England Journal of Medicine, 382*, 1199–1207. https://doi.org/10.1056/NEJMoa2001316

Li, L., Qin, L., Xu, Z., Yin, Y., Wang, X., Kong, B., et al. (2020b). Using artificial intelligence to detect COVID-19 and community-acquired pneumonia based on pulmonary CT: Evaluation of the diagnostic accuracy. *Radiology, 296*, E65–E71. https://doi.org/10.1148/radiol.2020200905

Loey, M., Smarandache, F., & Khalifa, N. E. M. (2020). Within the Lack of Chest COVID-19 X-ray Dataset: A Novel Detection Model Based on GAN and Deep Transfer Learning. *Symmetry, 12*, 651. https://doi.org/10.3390/sym12040651

Mercier, G., & Lennon, M. (2003). Support vector machines for hyperspectral image classification with spectral-based kernels. In *Proc. IGARSS, toulouse, France, July 21–25*.

Minaee, S., Kafieh, R., Sonka, M., Yazdani, S., & Soufi, G. J. (2020). Deep-Covid Predicting COVID-19 from chest X-ray images using deep transfer learning. *Medical Image Analysis*, P1–P9.

Mohammed, M. A., Abdulkareem, K. H., Al-Waisy, Alaa, S., Mostafa, S. A., Al-Fahdawi, S., Dinar, A. M., Alhakami, W., Baz, A., Al-Mhiqani, M. N., Alhakami, H., Arbaiy, N., Maashi, M. S., Mutlag, A. A., García-Zapirain, B., De La, T. D., & Isabel, De La T. (2020). Benchmarking methodology for selection of optimal COVID-19 diagnostic model based on entropy and TOPSIS methods. *IEEE Access, 8*, 99115–99131. https://doi.org/10.1109/ACCESS.2020.2995597

Mohammed, M. A., Abdulkareem, K. H., Garcia Zapirain, B., Mostafa, S. A., Maashi, M. S., Al Waisy, A. S., Ahmed Subhi, M., Mutlag, A. A., & Dac Nhuong, Le (2021). Comprehensive investigation of machine learning feature extraction and classification methods for automated diagnosis of COVID-19 based on X-ray images. *Computers, Materials & Continua, 66*(3). https://doi.org/10.32604/cmc.2021.012874

Narin, A., Kaya, C., & Pamuk, Z. (2020a). *Automatic detection of coronavirus disease (covid-19) using x-ray images and deep convolutional neural networks*. arXiv preprint arXiv: 2003.10849.

Narin, A., Kaya, C., & Pamuk, Z. (2020b). *Automatic detection of coronavirus disease (covid-19) using x-ray images and deep convolutional neural networks*. arXiv preprint arXiv: 2003.10849.

Nixon, M. S., & Aguado, A. S. (2013). *Feature extraction & image processing for computer vision* (3rd ed.). Elsevier Ltd.

Ozsahin, I., Sekeroglu, B., Musa, M. S., Mustapha, M. T., & UzunOzsahin, D. (2020). Review on diagnosis of COVID-19 from chest CT images using artificial intelligence. *Comput Math Methods Med*. https://doi.org/10.1155/2020/9756518, 2020-2021, 10.

Pathan, RK, Biswas, M, & Khandaker, M. U. (2020). Time series prediction of COVID-19 by mutation rate analysis using recurrent neural network-based LSTM model, chaos. *Solitons & Fractals, 138*, 110018.

Perez, L., & Wang, J. (2017). *The effectiveness of data augmentation in image classification using deep learning*. arXiv preprint arXiv:1712.04621.

Rahimzadeh, M., & Attar, A. (2020). A modified deep convolutional neural network for detecting covid-19 and pneumonia from chest x-ray images based on the concatenation of xception and resnet50v2. *Informatics in Medicine Unlocked*, 100360.

Rahmat, T., Ismail, A., & Aliman, S. (2018). Chest x-rays image classification in medical imageanalysis. *Applied Medical Informatics, 40*, 63–73.

Ramdas, K., Darzi, A., & Jain, S. (2020). 'Test, re-test, re-test': Using inaccurate tests to greatly increase the accuracy of COVID-19 testing. *Nature Medicine*, 1–2. https://doi.org/10.1038/s41591-020-0891-7

Rini, N. D. C., Rimuljo, H., et al. (2020). Detection of COVID-19 chest x-ray using support vector machine and convolutional neural network. *Communication Mathematics Biology Neuroscience*, 1–19. https://doi.org/10.28919/cmbn/4765, 2020.

Mahdy, L. N., Ezzat, K. A., Elmousalami, H. H., Ella, H. A., & Hassanien, A. E. (2020). Automatic x-ray COVID-19 lung image classification system based on multi-level thresholding and support vector machine. https://doi.org/10.1101/2020.03.30.20047787 (medRxiv preprint).

Shen, D., Wu, G., & Suk, H. (2017). Deep learning in medical image analysis. *Annual Review of Biomedical Engineering, 19*, 221–248.

Shi, F., et al. (2020). *Large-scale screening of covid-19 from community acquired pneumonia using infection size-aware classification*, Article 09860. arXiv :2003.

Shorten, C., & Khoshgoftaar, T. M. (2019). A survey on image data augmentation for deep learning. *Journal of Big Data, 6*(1), 60.

Thejeshwar, S. S., Chokkareddy, C., & Eswaran, K. (2020). *Precise prediction ofCOVID-19 in chest X-ray images using KE sieve algorithm*. https://doi.org/10.1101/2020.08.13.20174144.

Theodoridis, S., & Koutroumbas, K. (2003). *Pattern Recognition,2nded*. Elsevier, Academic Press.

Vapnik, V. N. (1998). *Statistical learning theory*. John-Wiley and Sons, Inc.

Waleed Salehi, A., Baglat, P., & Gupta, G. (2020). Review on machine and deep learning modelsfor the detection and prediction of coronavirus. *Materials Today Proceedings*. https://doi.org/10.1016/j.matpr.2020.06.245

Wang, S., et al. (2020a). *A deep learning algorithm using CT images to screen for Corona Virus Disease (COVID-19). medRxiv* (Vol. 24). Published online April, 2020.02.

Wang, L., Lin, Z. Q., & Wong, A. (2020b). COVID-net: A tailored deep convolutional neural network design for detection of COVID-19 cases from chest X-ray images. *Scientific Reports, 10*(1). https://doi.org/10.1038/s41598-020-76550-z

Wang, L., & Wong, A. (2020). *COVID-Net: A tailored deep convolutional neural network design for detection of COVID-19 cases from chest X-ray images*. arXiv preprint arXiv: 2003.09871.

World Health Organization. Q & A on coronaviruses (COVID-19). https://www.who.int/news-room/q-a-detail/q-a-coronaviruses. (Accessed 11 April 2020).

Worldometersinfo. (2020). The World meter website [Online], Available: https://www.worldometers.info/coronavirus/.

Xu, X., et al. (2020). *Deep learning system to screen coronavirus disease 2019 pneumonia*, Article 09334. arXiv:2002.

Yan, Z., & Yang, Y. (2014). A pplication of ECOCSVM sin remote sensing image classification, the international archives of photogrammetry. *Remote Sensing and Spatial Information Sciences40*, (2), 191.

Ying, S., Zheng, S., Li, L., Zhang, X., et al. (2020). Deep learning enables accurate diagnosis of novel coronavirus (COVID-19) with CT images. *IEEE/ACM Transactions on Computational Biology and Bioinformatics, 25*. https://doi.org/10.1109/tcbb.2021.3065361

Zhang, W. (2020). Imaging changes of severe COVID-19 pneumonia in advanced stage. *Intensive Care Medicine*, 1–3. https://doi.org/10.1007/s00134-020-05990-y

Zheng, Q., Yang, M., Tian, X., Jiang, N., & Wang, D. (2020). A full stage data augmentation method in deep convolutional neural network for natural image classification. *Discrete Dynamics in Nature and Society, 2020*, 1–11. https://doi.org/10.1155/2020/4706576

Zhong, Z., Jin, L., & Xie, Z. (2015). High performance offline handwritten Chinese character recognition using googlenet and directional feature maps. In *2015 13th international conference on document analysisand recognition (ICDAR)* (pp. 846–850). IEEE.

F.A. Saiz, I., 2020 Barandiaran; COVID-19 detection in chest X-ray images using aDeep learning approach,International Journal of Interactive Multimedia and Artificial Intelligence, Vol. 6, No- 2; P-11-14.

https://covid19.who.int/.

https://in.mathworks.com/help/stats/templatesvm.html. (Accessed 28 November 2019).

https://www.kaggle.com/andyczhao/covidx-cxr2. (Accessed July 2021).

https://www.kaggle.com/paultimothymooney/chest-xray-pneumonia. (Accessed July 2021).

https://www.nationalgeographic.com/science/2020/02/here-is-what-coronavirus-does-tothebody. (Accessed July 2021).

Bell, D., Murphy, A. COVID-19. Reference article, Radiopaedia.org. (accessed on 18 Feb 2022) https://doi.org/10.53347/rID-73913, 2022.